Progress In Electromagnetics Research Letters, Vol. 97, 35–43, 2021

An Online Extraction Method of Noise Source Impedance Based on Network Analyzer

Mingxing Du*, Yang Li, Qiqi Dai, and Ziwei Ouyang

Abstract—This paper presents an online noise source impedance extraction method based on network analyzer. Firstly, the composition scheme of the measurement method is given, the equivalent circuit model of the measurement system established, and the port structure of the equivalent circuit analyzed. Secondly, two known standard resistances are used to calibrate the measuring system and connecting wires. Finally, the passive device and DC/DC converter are used as the equipment to be tested, and the measurement results are compared with those of other methods and impedance analyzer. The comparison results show that the measurement method has high measurement accuracy and good temperature sensitivity.

1. INTRODUCTION

With the development of power electronic technology, the demand for high efficiency and power density is increasing. Silicon materials are being gradually replaced. Wide band gap semiconductor materials, including silicon carbide and gallium nitride, have more advantages than silicon. Therefore, wide gap power devices play an increasingly important role in power electronic systems [1–3]. The critical electric field, saturation drift velocity, electron mobility, and thermal conductivity of wide band gap semiconductor materials are higher than those of silicon materials [4]. However, higher switching frequency and power density make electromagnetic interference (EMI) more and more serious [5, 6]. The most effective way to reduce conducted emission is to use EMI filter composed of coupling inductance, capacitance, and resistance [7, 8]. If the design of EMI filter is not reasonable, it cannot effectively suppress EMI but will increase EMI, which will make the circuit work abnormally. In order to evaluate the performance of EMI filter, generally 50 Ω signal source is used as an interference source, and 50 Ω spectrum analyzer is used as a load to test the performance of EMI filter. However, there are few 50 Ω-50 Ω system in actual working conditions, which makes the actual performance inconsistent with the design value. Impedance mismatch is a common means to improve the performance of EMI filter [9]. Therefore, impedance relationship plays an important role in filter design. Therefore, measurement and analysis of noise source impedance is a prerequisite for designing EMI filter. At present, there are many methods to measure noise source impedance. In [10], a resonance method is proposed to measure the impedance of noise source. Inductors are added to the circuit to make it resonate with the EMI of the converter. Then the equivalent EMI impedance is derived from the resonant frequency and quality factor. This method is only a rough estimation of the noise source impedance. The measurement frequency band is narrow, and the practicability is poor. In [11], the insertion loss method is used to measure the impedance of noise sources. In this method, common mode choke and differential mode capacitor are connected in series to reduce the common mode and differential mode noise in the circuit. The noise source impedance is obtained by measuring the change of noise before and after the circuit. This measurement method has certain limitations. It is only applicable when the noise source impedance

Received 26 December 2020, Accepted 17 March 2021, Scheduled 23 March 2021
* Corresponding author: Mingxing Du (dumx@tjut.edu.cn).
The authors are with the Tianjin Key Laboratory of Control Theory & Applications in Complicated System, Tianjin University of Technology, Tianjin 300384, China.

is extremely large or extremely small. Therefore, this method has limited measurement conditions and poor practicability. The double current probe method is proposed in [12]. In this method, one current probe is used to inject interference into the circuit through coupling capacitance, and the other current probe is used to receive the interference in the circuit. Then, the spectrum analyzer is used to measure the current change before and after the interference injection in the circuit to obtain the noise source impedance. In this method, isolation inductance and coupling capacitance are added to the circuit when the current in the circuit is large, and the isolation inductance will saturate. When the current is small, the accuracy of the current probe is required to be higher. Impedance measurement is also very important in other fields, such as battery impedance online measurement technology under different frequency conditions [13–15]. These technologies or methods are not applicable in the field of noise source impedance measurement. In view of these shortcomings, this paper proposes a noise source impedance measurement method without the use of current probe. This method reduces the error caused by the accuracy of the current probe, so as to improve the measurement accuracy. The feasibility and accuracy of this method are verified by the test of passive and active components.

2. MEASURING METHOD

The measurement principle of this method is shown in Fig. 1. The measurement system consists of a network analyzer, two line impedance stabilization networks (LISNs), equipment under test (EUT), and the necessary connecting wires. The radio frequency (RF) signal is injected into the signal port of LISN1 through port1 of the network analyzer and then returns to port2 of the network analyzer through LISN2. Finally, the noise source impedance is obtained by combining measurement and calculation.

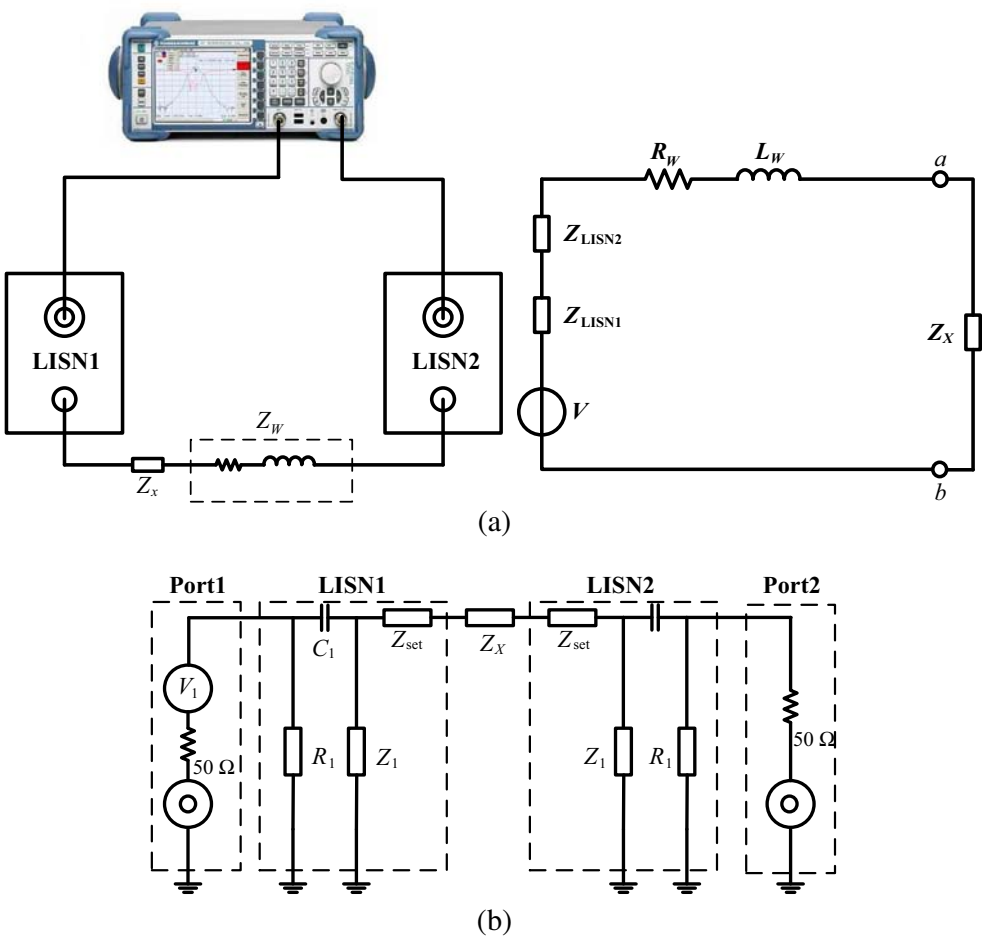

Figure 1. Measuring principle, (a) measuring circuit, (b) equivalent circuit.

Z_X is the impedance of the equipment under test, Z_W the impedance of the connecting wire, Z_{LISN1} the impedance of LISN1, and Z_{LISN2} the impedance of LISN2.

$$V = V_{a-b} + I_W \left(Z_{\text{LISN1}} + Z_{\text{LISN2}} + R_W + j\omega L_W\right) \tag{1}$$

$$\begin{aligned} V &= \left(Z_{\text{LISN1}} + Z_{\text{LISN2}} + R_W + j\omega L_W + Z_X\right) I_W \\ V &= \left(Z_{\text{setup}} + Z_X\right) I_W \end{aligned} \tag{2}$$

The voltage source can be expressed as:

$$V = \frac{Z_{\text{LISN1}}}{Z_{p1} + 50\,\Omega} V_1 \tag{3}$$

where V_1 represents the signal source voltage of port1 of network analyzer. $50\,\Omega$ represents the output impedance of port1; C_1 and R_1 are the capacitance and resistance of LISN respectively; Z_1 is the additional impedance generated by C_1, R_1, and power grid. The impedance Z_1 is very small and can be ignored, and the impedance of LISN is represented by Z_{LISN1} and Z_{LISN2}. Z_{port1} is the EMI measurement port impedance of LISN.

The equivalent circuit at $a - b$ can be regarded as a voltage source V and impedance Z_{setup} in series, so the impedance Z_X to be measured can be expressed as follows:

$$Z_X = \frac{V}{I_W} - Z_{\text{setup}} \tag{4}$$

The current can be expressed as:

$$I_W = \frac{V_{p2}}{Z_{T2}} \tag{5}$$

Z_{T2} is the transmission impedance, and V_{p2} is the signal voltage measured at the RF signal port of LISN2. Z_{p1} is the output impedance of LISN. The signal source V_1 can be expressed as:

$$V_1 = \left(\frac{50 + Z_{p1}}{Z_{p1}}\right) V_{p1} \tag{6}$$

By combining the above equations, we can obtain the following results:

$$Z_X = C\left(\frac{V_{p1}}{V_{p2}}\right) - Z_{\text{setup}} \tag{7}$$

V_{p1}/V_{p2} can be measured by vector network analyzer, because $V_{p1} = (S_{11} + 1)V_1$, $V_{p2} = S_{21}V_1$.

$$\frac{V_{p1}}{V_{p2}} = \frac{S_{11} + 1}{S_{21}} \tag{8}$$

The coefficient C and impedance Z_{setup} can be obtained by the following steps. Two standard resistors are selected as impedance Z_X to be measured, $R_{\text{std1}} = 100\,\Omega$, $R_{\text{std2}} = 1000\,\Omega$, and their respective V_{p1}/V_{p2} values are measured, respectively. An equation group with two unknowns C and Z_{setup} can be obtained by using Equation (6), and C and Z_{setup} can be obtained by solving the equations. After the values of C and Z_{setup} are obtained, Eq. (6) can be used to measure the unknown impedance Z_X.

$$\begin{cases} Z_X = |_{Z_X = R_{\text{std1}}} = C\left(\frac{V_{p1}}{V_{p2}}\right) - Z_{\text{setup}} \\ Z_X = |_{Z_X = R_{\text{std2}}} = C\left(\frac{V_{p1}}{V_{p2}}\right) - Z_{\text{setup}} \end{cases} \tag{9}$$

3. EXPERIMENTAL VERIFICATION

3.1. Passive Components

The resistances of $33\,\Omega$, $75\,\Omega$, $220\,\Omega$, $470\,\Omega$, $10000\,\Omega$, capacitances of 10 pF, 1 nF, and two resistive loads are selected as unknown impedance elements. The impedance of the whole measuring circuit is the

sum of the impedance to be measured and the impedance of the measurement system. The impedance influence of the measurement system has been removed from the above equation.

Firstly, the impedance magnitude and phase of these passive components are measured by impedance analyzer. Secondly, the method described in this paper and the method in [12] are used for measurement, and the results of three measurements are compared. The measurement results are shown in Fig. 2, Fig. 3, and Fig. 4. The solid lines in the figures are the curves measured by the impedance analyzer, the dashed lines the curves measured by the method described in this paper, and the short dotted lines the curves measured by using the method in [12]. It can be seen from the measurement results that in the frequency range of 150 kHz–30 MHz, the curve measured by this method is closer to that measured by impedance analyzer than the previous methods. However, the measurement curve in [12] is different from the other two methods in some frequency bands. Impedance analyzer can only be used for off-line measurement, which cannot reflect the online status of components. Under normal circumstances, the online impedance and off-line impedance of electrical equipment are very different. So it is necessary to accurately measure the noise source impedance of electrical equipment in the online state. The method described in this paper can be used not only for off-line measurement, but also for online measurement.

One of the most effective methods to reduce conducted emission is to use EMI filter composed of coupling inductance, capacitance, and resistance. The coupling inductance, capacitance, and resistance in an EMI filter may cause the temperature to rise due to the internal power loss. The temperature will

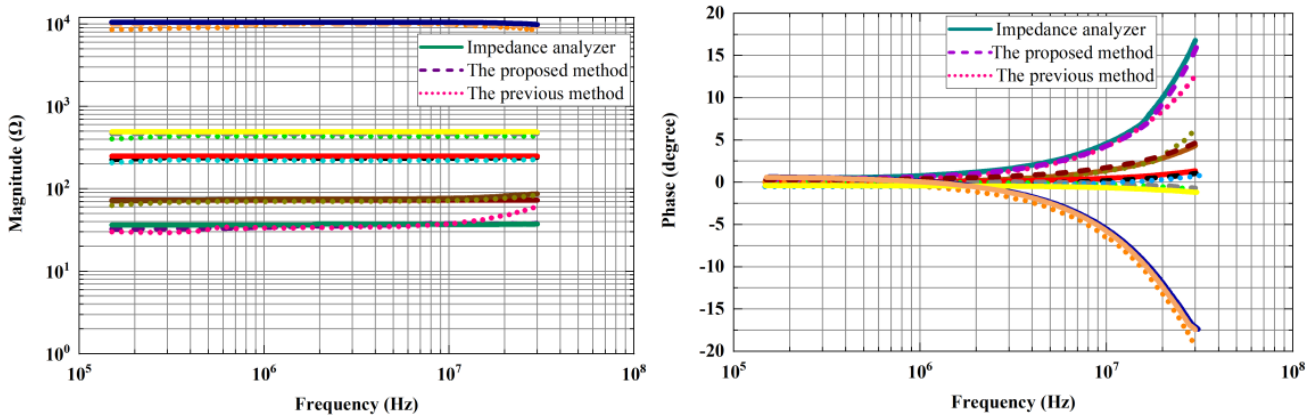

Figure 2. Resistance measurement results, (a) magnitude, (b) phase.

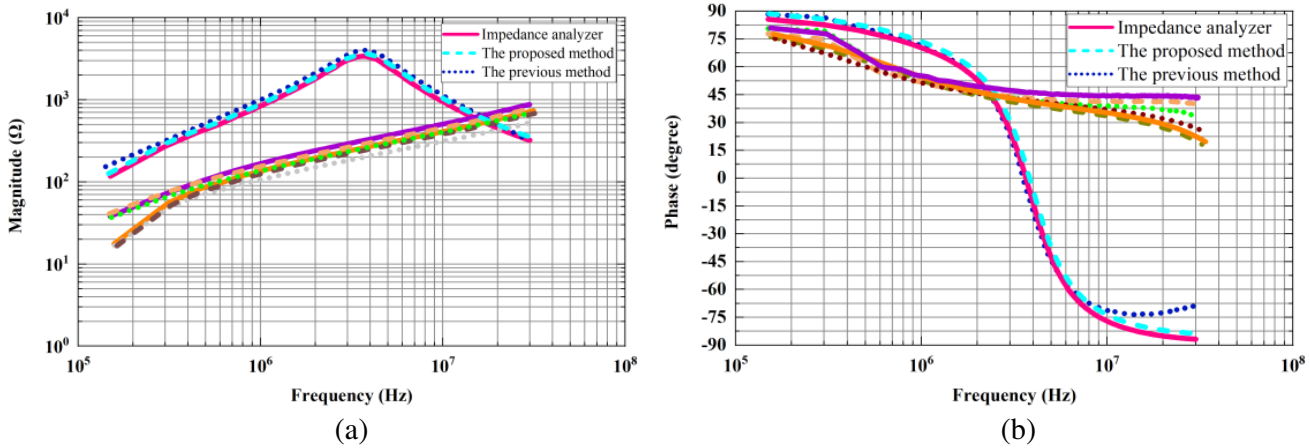

Figure 3. Inductance measurement results, (a) magnitude, (b) phase.

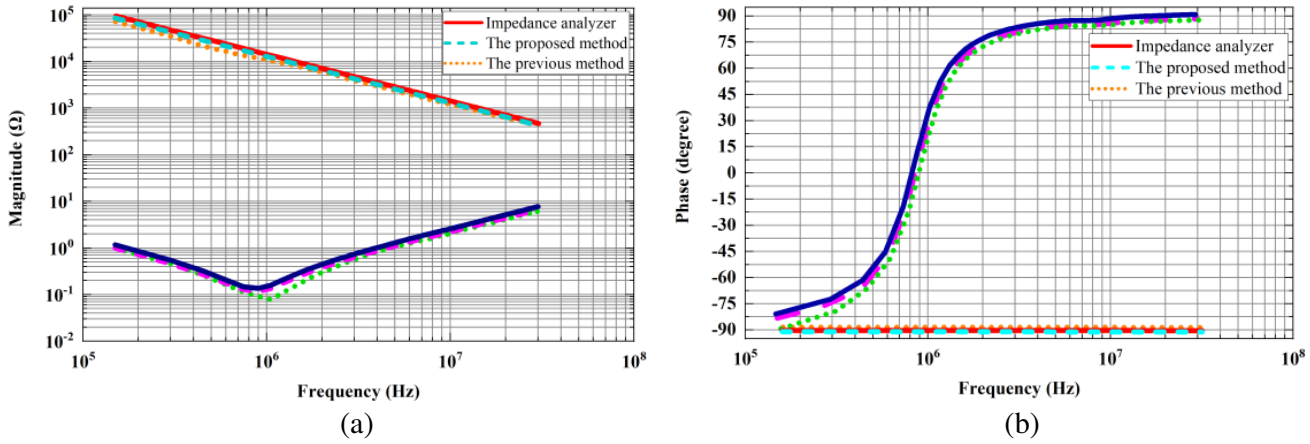

Figure 4. Capacitance measurement results, (a) magnitude, (b) phase.

greatly affect the resistance frequency characteristics of passive components, thus affecting the whole filter circuit.

3.1.1. Capacitance

In power electronic circuits, because of the exponential growth of switching frequency and switching loss, every element in the circuit will be heated. Capacitors of each material will have a limited operating temperature, beyond which the performance begins to decline. In order to verify the sensitivity of the proposed method under different temperature conditions, taking the impedance frequency characteristics of capacitor under the condition of temperature change as an example, the capacitors of plastic and ceramic materials are put into the constant temperature and humidity chamber, and the experimental conditions are simulated by adjusting the set temperature of the constant temperature and humidity chamber. In order to ensure the accuracy of the temperature in the constant temperature and humidity chamber, the internal temperature is stable for 30 minutes before the experimental measurement is performed. The measurement results are shown in Fig. 5 and Fig. 6.

It can be seen from Fig. 5 and Fig. 6 that when the temperature in the constant temperature and humidity chamber increases from 25°C to 100°C, the impedance of the two capacitors changes little. When the temperature increases from 25°C to 100°C, the resonant frequency of 470 nF capacitor increases from 0.83 MHz to 1.30 MHz. When the temperature is lower than the first resonant frequency,

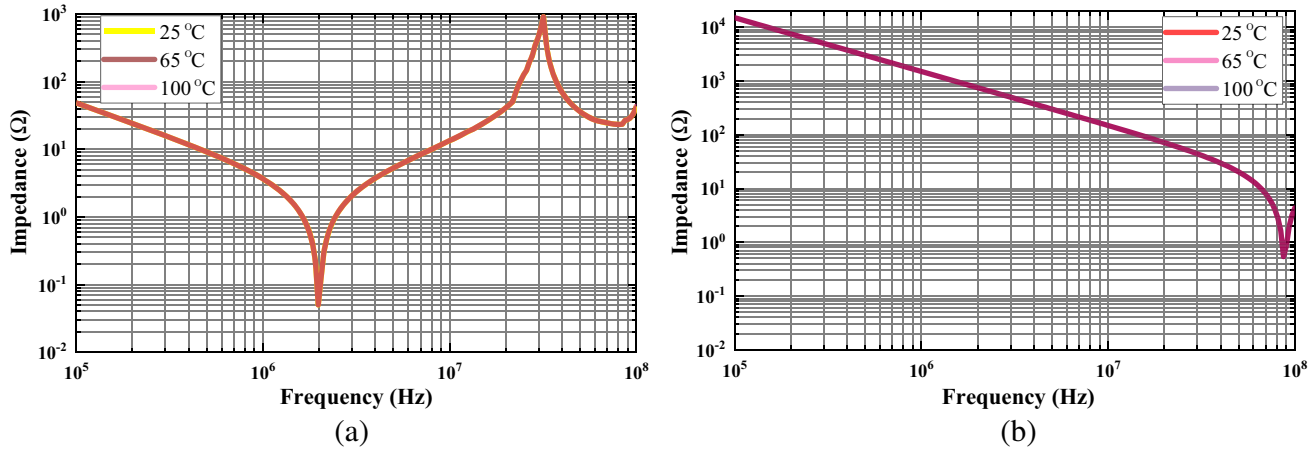

Figure 5. Impedance magnitude of (a) 33 nF and (b) 100 pF plastic capacitors at different temperatures.

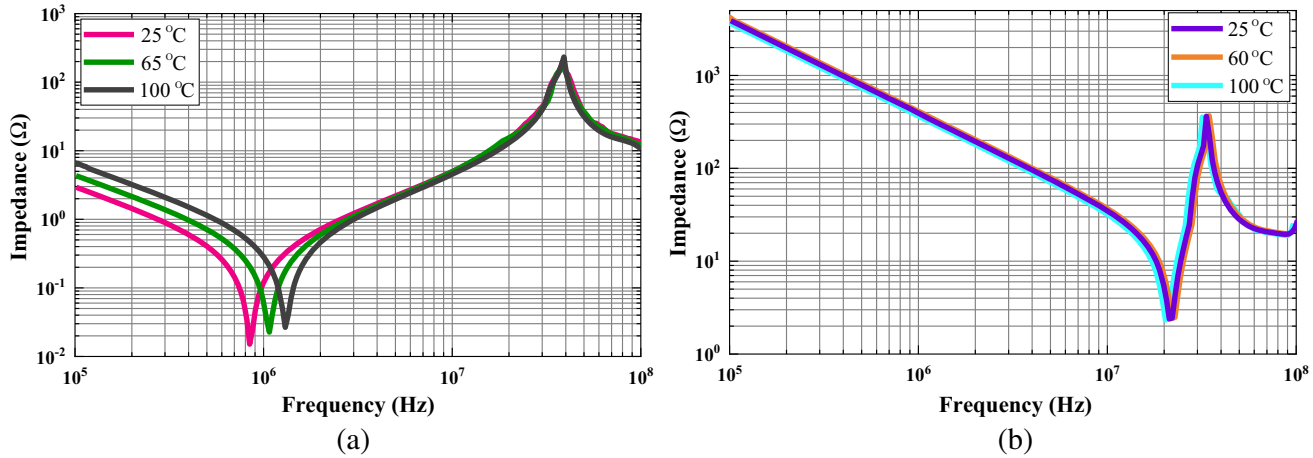

Figure 6. Impedance magnitude of (a) 470 pF and (b) 470 pF ceramic capacitors at different temperatures.

the impedance decreases obviously. When the temperature rises from 25°C to 100°C, the impedance of 470 pF capacitance changes little in the whole measurement frequency range. Therefore, it can be concluded that the larger the capacitance (ceramic capacitance) is, the greater the influence of temperature change is. In most of the literature, the impedance of passive components is measured by impedance analyzer. If the impedance analyzer is used to study the resistance frequency characteristics of capacitor under temperature change, the effect is not obvious. Even if the temperature range is large, the impedance change of capacitor is not obvious, that is to say, this method is not sensitive to temperature. However, the method in this paper is based on S-parameter, which is sensitive to temperature, so we can use this characteristic to study the influence of temperature on capacitor impedance.

3.1.2. Coupling Inductance

The coupling inductor will change the temperature due to many factors, such as power loss and the change of ambient temperature. However, the change of temperature will affect the performance of the coupled inductor, thus affecting the performance of EMI filter [15]. By identifying the temperature sensitivity of the coupled inductor, the actual performance of the coupled inductor can be predicted. In order to determine the specific influence of temperature change on the coupled inductor, the magnetization impedance, common mode impedance, differential mode impedance, and leakage impedance of the coupling inductor are measured by the method described in this paper. This method can not only verify the sensitivity of the proposed method to the change of experimental environment, but also study the impedance frequency characteristics of the coupled inductor under temperature change. The measurement environment is the same as that of capacitor, and the measurement curve is shown in Fig. 7.

As can be seen from Fig. 7(a), when the temperature rises from 25°C to 100°C, the magnetization impedance increases. This is because the sensitivity of magnetization impedance to temperature is related to the complex permeability of the magnetic core used. The complex permeability is very sensitive to the change of temperature, so the impedance is greatly affected by temperature. Similar to the magnetization impedance, the common mode impedance increases when the temperature increases from 25°C to 100°C. This is also related to the complex permeability of the core.

It can be seen from Fig. 7(c) and Fig. 7(d) that the magnitude of differential mode impedance and leakage impedance does not change with temperature. This is because in both cases, the magnetic flux generated in the ferrite core is equal to zero. However, the leakage impedance is generated by the leakage flux in the core. The composite permeability of these two cases is related to the air permeability ($\mu_r = 1$), and the air permeability has nothing to do with the temperature, so the two kinds of impedances do not change with temperature.

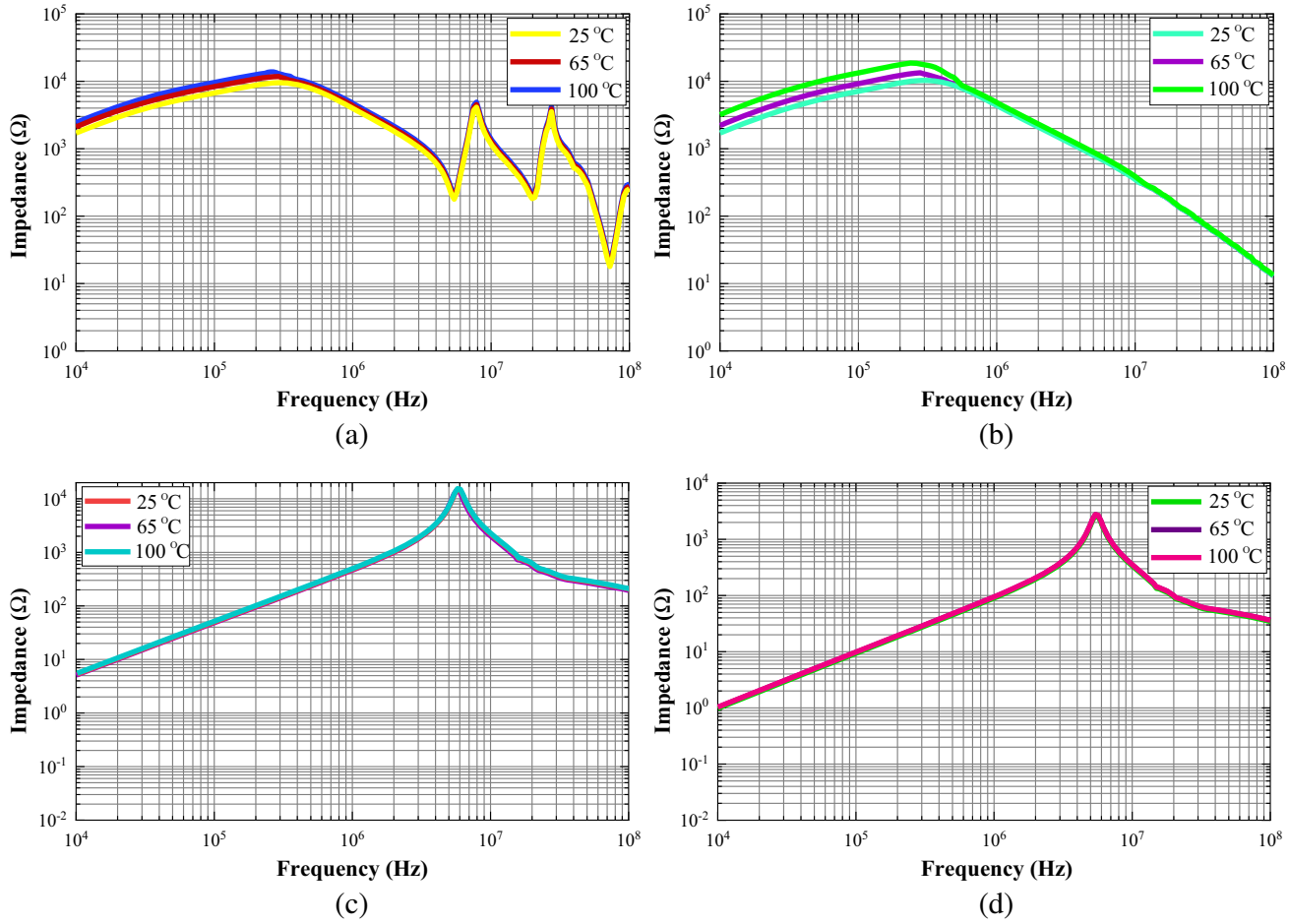

Figure 7. Test results of coupling inductance, (a) magnetization impedance; (b) common mode impedance; (c) differential mode impedance; (d) leakage impedance.

In most of the literature, the impedance of passive components is measured by impedance analyzer. If the impedance analyzer is used to study the impedance frequency characteristics of coupling inductor under temperature change, the effect is not obvious, because even if the temperature range is large, the impedance change of coupling inductor is not obvious, that is to say, this method is not sensitive to temperature. However, the method proposed in this paper is based on S-parameter, which is sensitive to temperature. Therefore, this characteristic can be used to study the influence of temperature on the impedance of coupled inductor.

3.2. Active Component

In order to verify the effectiveness of this method in noise impedance measurement, a DC/DC converter is selected as the tested device. The DC/DC converter is powered by GWINSTEK PSW 30-108 programmable DC power supply. The working voltage of DC/DC converter is 24 V, and the output voltage is 18 V. The DC/DC converter supplies power to a load.

As shown in Fig. 8, the DC/DC converter uses two wires to connect to the DC power supply. The RF signal from port1 of the vector network analyzer is injected into the circuit under test through the RF signal port of LISN1. The RF signal in the circuit returns to port2 of the vector network analyzer through the RF signal port of LISN2. Based on the analysis in Section 2, the coefficient C and Z_{setup} of each frequency point have been calculated. Therefore, the noise impedance of DC/DC converter can be obtained by calculating the value of V_{p1}/V_{p2}.

In order to verify the accuracy of the online measurement, the measurement results are shown in

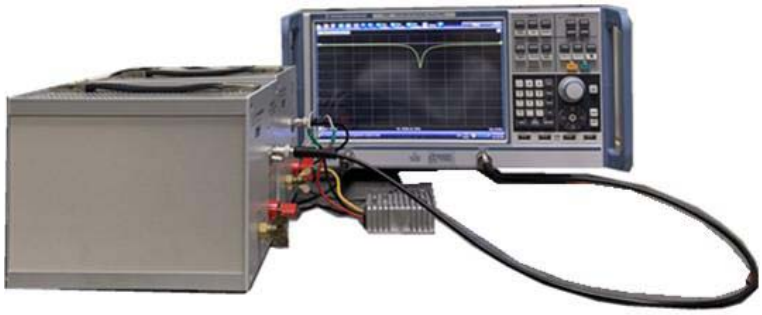

Figure 8. Online measurement system of DC/DC converter noise impedance.

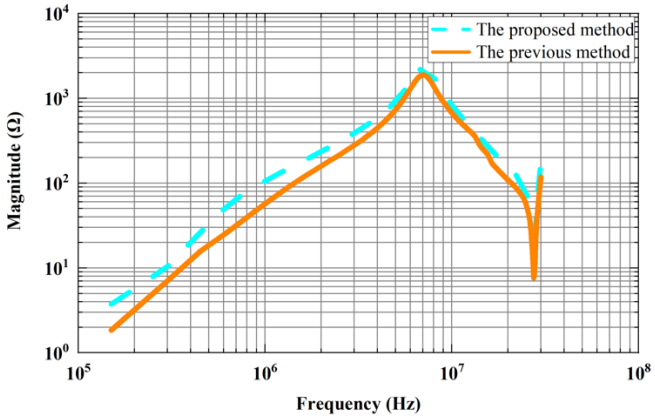

Figure 9. Noise impedance curve of DC/DC converter.

Fig. 9. In Fig. 9, the solid line is the measurement result of the method described in this paper, and the dotted line is the measurement result of the existing method. It can be seen from Fig. 9 that the trends of impedance curves measured by the two methods are very close, which verifies the effectiveness and feasibility of the method.

4. CONCLUSIONS

In this paper, an online noise source impedance extraction method is proposed. Compared with the previous measurement methods, this method does not need to use the current probe. The previous methods have higher requirements on the accuracy of the current probe, which reduces the error caused by the accuracy of the current probe, so as to improve the measurement accuracy, reduce the current probe calibration, and greatly reduce the complexity of the experiment. At the same time, the measurement bandwidth of this method is also improved, and the effective bandwidth is increased by more than half. In this paper, different resistances, capacitances, and inductance loads are measured, and the measurement results are compared with those of impedance analyzer and Reference [12]. The experimental results show that the measurement results of the method described in this paper are closer to those of the impedance analyzer than the previous methods. The measurement method in [12] is different from the other two methods in some frequency bands. In order to verify the sensitivity of the proposed method to the change of experimental conditions, the impedance frequency characteristics of capacitor and coupling inductor under different temperature are measured. The measurement results show that the method has good temperature sensitivity. Finally, the DC/DC converter in working state is measured, and the measurement results are compared with those of the previous methods. The trends of the measurement curves of the two methods are basically the same, but the impedance magnitude changes in some frequency bands.

ACKNOWLEDGMENT

This work was supported in part by the Tianjin Municipal Science and Technology Project (No. 20YDTPJC00510) and the "New Energy Vehicle" Key Special Project of the National Key Research and Development Plan (No. 2017YFB0102500).

REFERENCES

1. Millán, J., P. Godignon, X. Perpiñà, A. Pérez-Tomás, and J. Rebollo, "A survey of wide bandgap power semiconductor devices," *IEEE Transactions on Power Electronics*, Vol. 29, No. 5, 2155–2163, May 2014.
2. Jones, E. A., F. F. Wang, and D. Costinett, "Review of commercial GaN power devices and GaN-based converter design challenges," *IEEE Journal of Emerging and Selected Topics in Power Electronics*, Vol. 4, No. 3, 707–719, Sept. 2016.
3. Lemmon, A. N., R. Cuzner, J. Gafford, R. Hosseini, A. D. Brovont, and M. S. Mazzola, "Methodology for characterization of common-mode conducted electromagnetic emissions in wide-bandgap converters for ungrounded shipboard applications," *IEEE Journal of Emerging and Selected Topics in Power Electronics*, Vol. 6, No. 1, 300–314, Mar. 2018.
4. Zhang, B. and S. Wang, "A survey of EMI research in power electronics systems with wide-bandgap semiconductor devices," *IEEE Journal of Emerging and Selected Topics in Power Electronics*, Vol. 8, No. 1, 626–643, Mar. 2020.
5. Kovačević, I. F., T. Friedli, A. M. Müsing, and J. W. Kolar, "3-D electromagnetic modeling of parasitics and mutual coupling in EMI filters," *IEEE Transactions on Power Electronics*, Vol. 29, No. 1, 135–149, Jan. 2014.
6. Domínguez-Palacios, C., J. B. Mendez, and M. A. M. Prats, "Characterization of three-phase common-mode chokes at high frequencies," *IEEE Transactions on Power Electronics*, Vol. 33, No. 8, 6471–6475, Aug. 2018.
7. Lee, C. K., D. Xu, B. M. H. Pong, S. Kiratipongvoot, and W. M. Ng, "A three-winding common mode inductor," *IEEE Transactions on Power Electronics*, Vol. 32, No. 7, 5180–5187, Jul. 2017.
8. Xing, L. and J. Sun, "Conducted common-mode EMI reduction by impedance balancing," *IEEE Transactions on Power Electronics*, Vol. 27, No. 3, 1084–1089, Mar. 2012.
9. Luo, F., D. Boroyevich, and P. Mattavelli, "Improving EMI filter design with in circuit impedance mismatching," *2012 Twenty-Seventh Annual IEEE Applied Power Electronics Conference and Exposition (APEC)*, 1652–1658, Orlando, FL, 2012.
10. Schneider, L. M., "Noise source equivalent circuit model for off-line converters and its use in input filter design," *1983 IEEE International Symposium on Electromagnetic Compatibility*, 1–9, Arlington, VA, USA, 1983.
11. Zhang, D., D. Y. Chen, M. J. Nave, and D. Sable, "Measurement of noise source impedance of off-line converters," *IEEE Transactions on Power Electronics*, Vol. 15, No. 5, 820–825, Sept. 2000.
12. See, K. Y. and J. Deng, "Measurement of noise source impedance of SMPS using a two probes approach," *IEEE Transactions on Power Electronics*, Vol. 19, No. 3, 862–868, May 2004.
13. Howey, D. A., P. D. Mitcheson, V. Yufit, G. J. Offer, and N. P. Brandon, "Online measurement of battery impedance using motor controller excitation," *IEEE Transactions on Vehicular Technology*, Vol. 63, No. 6, 2557–2566, Jul. 2014.
14. Huang, W. and J. A. Abu Qahouq, "An online battery impedance measurement method using DC-DC power converter control," *IEEE Transactions on Industrial Electronics*, Vol. 61, No. 11, 5987–5995, Nov. 2014.
15. Abu Qahouq, J. A., "Online battery impedance spectrum measurement method," *2016 IEEE Applied Power Electronics Conference and Exposition (APEC)*, 3611–3615, Long Beach, CA, 2016.